ACS Photonics

Letter

pubs.acs.org/journal/apchd5

Quantifying the Plasmonic Character of Optical Excitations in Nanostructures

Luca Bursi,[†,‡] Arrigo Calzolari,[*,‡] Stefano Corni,[*,‡] and Elisa Molinari[†,‡]

[†]Dipartimento di Fisica, Informatica e Matematica, Università di Modena e Reggio Emilia, I-41125 Modena, Italy

[‡]Istituto Nanoscienze CNR-NANO-S3, I-41125 Modena, Italy

Supporting Information

ABSTRACT: The microscopic definition of plasmons in nanosystems is a tremendous challenge. Any sharp distinction of the excitation nature (nonplasmonic vs plasmonic) becomes blurred at the nanoscale, where quantum effects become important. Here we introduce the concept of *plasmonicity index*, i.e., a direct measure of the plasmonic character of the optical excitations in nanosystems. Its definition is based on a rigorous theoretical derivation, which leads to the physically sound result that the plasmonicity index is related to the capability of enhancing locally an applied electromagnetic radiation. The proposed expression is general and can be applied to any finite system. We show its usefulness in modeling metallic nanoparticles, prototypical C-based molecules, and paradigmatic hybrid systems, starting from first-principles calculations, based on (TD)DFT. Our results represent a step forward in the fundamental understanding of what a plasmon is in nanometer-sized particles and molecular systems.

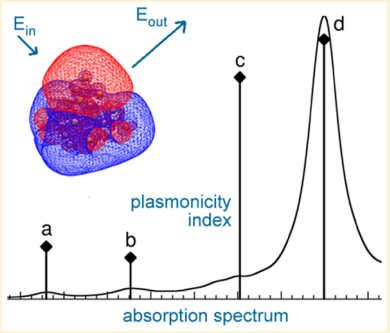

KEYWORDS: *definition of plasmons, atomistic modeling of optical excitations, molecular plasmons, metal clusters, graphene nanostructures*

Localized surface plasmon resonances in nanostrucures interact strongly with light, allowing the confinement of electromagnetic energy down to deep subwavelength regions.[1,2] This, together with their easy tunability,[3] robustness,[4] and field enhancement properties,[5] provides a powerful tool to manipulate light at the nanoscale, below the diffraction limit. Thus, plasmons have become of paramount importance for a wide range of applications[6−8] spanning from light harvesting[9] to biosensing.[10] In general terms, plasmons can be defined as electronic collective excitations that arise when the Coulomb interaction between excited states is switched on.[11] However, their theoretical description at the microscopic level is still an open and controversial issue.[12] In large nanoparticles optical and plasmonic properties are generally described by electrodynamics of continuous media, exploiting semiclassical models of the frequency-dependent dielectric function,[13] and the identification of plasmons is straightforward. This description has been very useful for designing applications, but fails to convey a microscopic understanding of what plasmons are. Nanoparticles and their excitations are composed of electrons and nuclei like ordinary molecules. Therefore, it must be possible to understand their excited states, including plasmons, in terms of the same elementary electron and hole excitations routinely used to interpret molecular excited states. Notably, such a microscopic description is mandatory when the system size reaches 1−2 nm, where the dielectric description breaks down and quantum finite-size effects[2,14] as well as the details of the atomic structure[15,16] play a crucial role. However, at the nanoscale, single-particle and plasmonic excitations are intrinsically mixed,[17,18] and how to recognize a plasmonic excitation is still an unsolved problem.

A few approaches have been recently proposed attempting to classify the plasmonic character of the excitations of nanosystems.[11,19−25] In particular, Bernadotte et al.[11] formulated, in the framework of time-dependent density-functional theory (TDDFT), a scaling approach based on the different dependence of the energies of the excitations of nanosystems on the Coulomb kernel. Along this line, Krauter et al.[25] extended the scaling scheme to selected first-principles wavefunction-based approaches.

All the aforementioned proposals lack a simple quantification of the relative plasmonic character of the electronic excitations. In this work, we present an approach based on the quantitative assessment of the plasmonic character of the excitations, which allows us to overcome this problem. To this end, we define an index that quantifies the *plasmonicity* of a given excitation. In particular, we focus on light-induced optical excitations, which are the ones typically of interest in nanosystems.

When a monochromatic external scalar potential $v_{ext}(\boldsymbol{r}, \omega)$ is applied to a physical system, its equilibrium charge density changes as a response to the perturbation. This modification is the induced charge density $n'(\boldsymbol{r}, \omega) = \int \chi(\boldsymbol{r}, \boldsymbol{r}', \omega)\, v_{ext}(\boldsymbol{r}', \omega)\, d^3\boldsymbol{r}'$, which in turn generates an induced potential $v_{ind}(\boldsymbol{r}, \omega) = \int f_{Coul}(\boldsymbol{r} - \boldsymbol{r}')\, n'(\boldsymbol{r}', \omega)\, d^3\boldsymbol{r}'$. The external density response function χ and the Coulomb kernel $f_{Coul}(\boldsymbol{r} - \boldsymbol{r}') = \frac{1}{|\boldsymbol{r} - \boldsymbol{r}'|}$ have

Received: December 1, 2015
Published: March 23, 2016

DOI: 10.1021/acsphotonics.5b00688
ACS Photonics 2016, 3, 520−525

been introduced. The superposition of the external and the induced potential gives the total potential $v_{tot}(\boldsymbol{r}, \omega) = v_{ext}(\boldsymbol{r}, \omega) + v_{ind}(\boldsymbol{r}, \omega)$, and n' can be rewritten in terms of v_{tot} through the irreducible response function χ_0 as $n'(\boldsymbol{r}, \omega) = \int \chi_0(\boldsymbol{r}, \boldsymbol{r}', \omega) v_{tot}(\boldsymbol{r}', \omega)\, d^3\boldsymbol{r}'$. From the previous expressions, the well-known Dyson-like integral equation for the response functions can be obtained:[26]

$$\chi(\boldsymbol{r}, \boldsymbol{r}', \omega) = \chi_0(\boldsymbol{r}, \boldsymbol{r}', \omega) + \iint \chi_0(\boldsymbol{r}, \boldsymbol{r}''', \omega) f_{Coul}(\boldsymbol{r}''' - \boldsymbol{r}'') \chi(\boldsymbol{r}'', \boldsymbol{r}', \omega)\, d^3\boldsymbol{r}'''\, d^3\boldsymbol{r}'' \quad (1)$$

Notably, the TDDFT equivalent of the above equation contains also the exchange−correlation (xc) kernel f_{xc}, in addition to f_{Coul}. Since plasmons are obtained already at the level of theory represented by eq 1, f_{xc} is not required to figure out the expression of the index, and we do not include it in the following derivation. We expand this point later in the text and in the Supporting Information (SI).

The poles ω_ξ of the external response function, which correspond to the zero modes of χ^{-1},

$$\int \chi^{-1}(\boldsymbol{r}, \boldsymbol{r}', \omega_\xi) \rho_\xi(\boldsymbol{r}')\, d^3\boldsymbol{r}' = 0 \quad (2)$$

are the frequencies of the electronic excitations of the system. In eq 2, ρ_ξ is the transition density for the ξ excitation formally defined as $\rho_\xi(\boldsymbol{r}') = \langle \xi | \Psi^\dagger(\boldsymbol{r}')\, \Psi(\boldsymbol{r}') | 0 \rangle$, where $|\xi\rangle$ and $|0\rangle$ are the excited and ground states, while $\Psi^\dagger$ and Ψ are the electron creation and annihilation field operators,[26] respectively.

In macroscopic systems, it is convenient to introduce the dielectric function ε.[27,28] Equation 2 can thus be rewritten as $\iint \varepsilon(\boldsymbol{r}, \boldsymbol{r}'', \omega_\xi)\, \chi_0^{-1}(\boldsymbol{r}'', \boldsymbol{r}', \omega_\xi)\, \rho_\xi(\boldsymbol{r}')\, d^3\boldsymbol{r}''\, d^3\boldsymbol{r}' = 0$. Considering the above equations and according to the typical classification adopted in solid-state physics,[11,26,29] the poles of χ can be divided into two types: (i) those corresponding to the zero modes of ε, identified as plasmons, and (ii) those originated from the poles of χ_0, hereafter called nonplasmonic excitations.

Albeit physically intuitive, this classification is not directly applicable to molecules and nanoparticles, for which the concept of ε is not straightforward. To maintain a physical link between plasmonic character and optical quantities, here we provide a fully microscopic derivation. From eq 1 we obtain the relation

$$\chi^{-1}(\boldsymbol{r}, \boldsymbol{r}', \omega) = \chi_0^{-1}(\boldsymbol{r}, \boldsymbol{r}', \omega) - f_{Coul}(\boldsymbol{r} - \boldsymbol{r}') \quad (3)$$

Substituting eq 3 in eq 2, we have

$$\int \chi_0^{-1}(\boldsymbol{r}, \boldsymbol{r}', \omega_\xi) \rho_\xi(\boldsymbol{r}')\, d^3\boldsymbol{r}' - v_{ind\rho}(\boldsymbol{r}, \omega_\xi) = 0 \quad (4)$$

where $v_{ind\,\rho}$ is the induced potential generated by ρ. In the same spirit of the analysis done above, we can now classify the character of the excitation looking at the zeros of eq 4, which includes only microscopic quantities. Nonplasmonic excitations correspond to the poles of the irreducible response function, i.e., to zero modes of χ_0^{-1}, and therefore at the frequency of an excitation of this kind, the first term of eq 4 vanishes. Since eq 4 still holds, also the induced potential in the case of a nonplasmonic excitation should in principle vanish. Plasmons, instead, do not correspond to zero modes of χ_0^{-1}, and thus the first term of eq 4 does not vanish, at the frequency of a plasmonic excitation. Therefore, the potential induced by a plasmon should remain finite, in order to satisfy eq 4. The measure of how much the induced potential deviates from 0 can be interpreted as the measure of the plasmonic character of the excitation. Among the many possible measures of how much $v_{ind\,\rho}$ deviates from 0, we choose its L^2 norm. We therefore introduce a *plasmonicity index*, η_P, for the excitation ξ as

$$\eta_P = \frac{\int |v_{ind\rho}(\boldsymbol{r}, \omega_\xi)|^2 d^3\boldsymbol{r}}{\int |\rho_\xi(\boldsymbol{r})|^2 d^3\boldsymbol{r}} = \frac{\int \left| \int \frac{\rho_\xi(\boldsymbol{r}')}{|\boldsymbol{r} - \boldsymbol{r}'|} d^3\boldsymbol{r}' \right|^2 d^3\boldsymbol{r}}{\int |\rho_\xi(\boldsymbol{r})|^2 d^3\boldsymbol{r}} \quad (5)$$

In light of the above considerations, the higher η_P is the more plasmonic is the excitation of frequency ω_ξ. The direct relation between the plasmonic nature of an excitation and the intensity of the relative induced potential is physically sound, as plasmons are typically connected with the local enhancement of the electromagnetic field. By definition, η_P is also discriminating plasmons by states with double excitation character: the latter have a small transition density (since this is obtained by a single-particle operator) and thus has a small η_P. At any rate, in this work η_P will be calculated by means of TDDFT linear response theory with a frequency-independent kernel that does not account for double excitations. We choose the normalization of η_P in eq 5 in order to properly define an approximated η_P, called $\tilde{\eta}_P$ in the following, which can be obtained from the results of a TDDFT linear response calculation, as detailed in the Methods section. In fact, all the numerical results presented later refer to $\tilde{\eta}_P$, although a direct calculation of η_P is also possible from the results of the Casida TDDFT equation. We also explored an alternative normalization for the plasmonicity index. It identified the same excitations as plasmonic, although gave a less detailed picture of the weakly plasmonic excitations. The alternative normalization and the comparison of results between the two definitions is reported in the SI.

This definition of the plasmonicity index is general and not restricted to any specific system or numerical implementation, being based only on the intimate interaction of matter with electromagnetic fields at the nanoscale. In the present case, we calculate the plasmonicity index for a few paradigmatic systems, starting from a TDDFT simulation of the optical excitations. We considered a linear Na_{20} chain and a tetrahedral Ag_{20} cluster as model plasmonic metallic nanosystems,[11,30,31] a naphthalene molecule as an example of a molecular system that hosts "molecular plasmons",[19,22,32,33] and a coupled system composed of a tetrahedral Ag_{20} cluster and a pyridine molecule, which represents a prototypical hybrid system[34] mixing plasmonic and molecular portions.

Starting from the first-principles results, we computed the plasmonicity index defined by eq 5. When TDDFT methods are used, eq 1 also contains the xc kernel, in addition to the Coulomb kernel. Since the lower level Random Phase Approximation (RPA) theory (i.e., no xc) does predict plasmons, the effects contained in the xc kernel cannot be decisive in signaling the plasmonic nature of a transition. Thus, $v_{ind\,\rho}$, the key quantity in RPA, maintains its central role in TDDFT as well, and the plasmonicity index is still written as in eq 5; see the SI. Obviously, the realism of the description and thus the quality of the plasmonicity index do depend on the choice of the xc kernel (incidentally, TD Hartree−Fock can be considered as a special case of this choice), but only indirectly via the transition density, as for any TDDFT calculation.

Na_{20}. In Figure 1, the TDDFT absorption spectrum (black solid line) of the Na_{20} chain (the atomic structure is shown as

DOI: 10.1021/acsphotonics.5b00688
ACS Photonics 2016, 3, 520−525

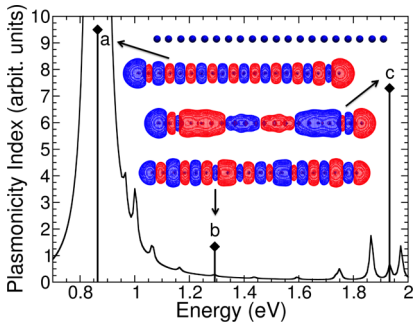

Figure 1. TDDFT absorption spectrum averaged over the three spatial polarizations (in arbitrary units) of the Na_{20} chain (black line) and plasmonicity index (black diamonds and vertical lines) computed for selected peaks in the spectrum, labeled from a to c. Insets show the atomic structure of the chain and a few selected isosurface plots of the imaginary part of the TDDFT response charge density, corresponding to an external field polarized along the longitudinal direction of the chain and computed at the frequency of the peak.

an inset) is dominated by an intense peak labeled with a in the low-energy region. By using the same example as a benchmark, Bernadotte et al.[11] have investigated the plasmonic properties of this system on the basis of the comparison with the 1D free-electron gas plasmons, identifying the excitations here labeled a and c as plasmons and peak b as nonplasmonic. We computed the TDDFT response charge density and the plasmonicity index for peaks a−c (Figure 1). Indeed, we performed such analysis for all the optically active peaks (more than 30) in the low-energy range, and then we selected the most significant ones to ensure the readability of the result. Some more excitations are shown in the SI. The response charge densities of a and b tend to be localized at the edges of the chain, leaving a charge depletion in the center, thus showing a dipolar character. This feature may indicate a plasmon resonance in a quasi-1D molecular system,[22] but it is still an ambiguous indication, and it is not always sufficient to discriminate the plasmonic character. By plotting, instead, the values of the plasmonicity index (black diamonds in Figure 1) as a function of the energy, we obtain a "plasmonic spectrum" (black vertical lines in Figure 1) that spots plasmonic and nonplasmonic excitations. First of all, we note that the value of η_P is not trivially related to the oscillator strength of the peak. In particular, peak c is almost as plasmonic as peak a, despite that its oscillator strength is negligible in comparison. Second, the plasmonicity index of peaks a and c is markedly greater than that of peak b, identifying those excitations as plasmonic, in agreement with the independent assignment of Bernadotte et al.[11] This is an important finding, as it shows that η_P correctly reproduces the results of more complex approaches, such as the scaling scheme, when they are applicable. Regarding the comparison between our results and those of Bernadotte et al.,[11] we note that the differences in the energies of the peaks are due to the different xc kernels adopted. Furthermore, while we analyze induced charge densities, they inspect transition densities. This, together with the different xc kernels and the different choice of isosurface values for plotting, justifies some discrepancies in the density figures.

Naphthalene. Now we consider a carbon-based molecular system where only a few transitions can be observed in the low-energy region of absorption. The spectrum of naphthalene in Figure 2 (where also the molecular structure is displayed as an inset) shows two bands, namely, the most intense peak b and

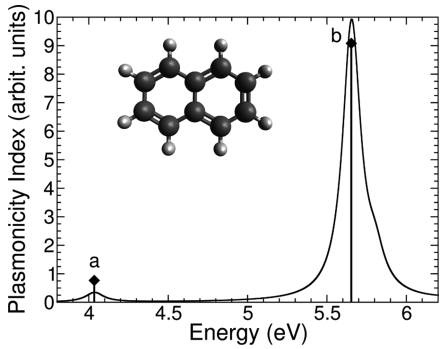

Figure 2. TDDFT absorption spectrum averaged over the three spatial polarizations (in arbitrary units) of naphthalene (black line) in the low-energy region and plasmonicity index (black diamonds and vertical lines) computed for peaks a and b in the spectrum. The molecular structure is shown as an inset.

the weaker peak a at lower energy.[19,22] We have studied the electronic, optical absorption, plasmonic, and local field enhancement properties of this system elsewhere[22] with the same computational procedure, and we refer to that for further details. In previous works, b has been identified as a molecular plasmon.[19,22] The plasmonicity index analysis is in agreement with the picture just described, showing its usefulness also for truly nonmetallic molecular systems. Notably, by comparing the plasmonicity index of peaks a and b, we conclude that the excitation b is more plasmonic than the excitation a. This is confirmed by the inspection of the induced charge densities,[22] and it is a posteriori conforming with intuition. Nevertheless, this does not mean that peak a is nonplasmonic: indeed, it could be a transverse molecular plasmon with the contribution of just one (i.e., HOMO → LUMO) leading single-particle transition.[25]

Ag_{20}. η_P is especially useful in the characterization of the plasmonic properties of systems where the visual inspection of the response charge density does not give straightforward indications, as the tetrahedral Ag_{20} cluster (the atomic structure is shown in the inset of Figure 3). The latter is a well-known plasmonic system,[11,31,34] despite its small number of atoms. An intense peak dominates the low-energy region of the absorption spectrum of this cluster (see Figure 3), and, according to Bernadotte et al.,[11] in correspondence with that peak, plasmonic and nonplasmonic excitations mix, not allowing an easy identification of their character. In this case, the most

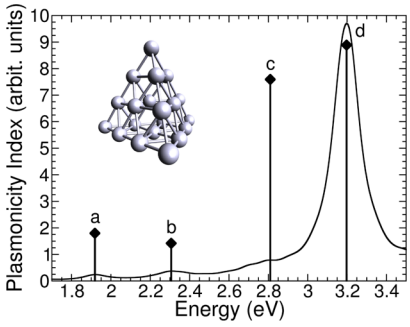

Figure 3. TDDFT absorption spectrum averaged over the three spatial polarizations (in arbitrary units) of the Ag_{20} cluster (black line) in the low-energy region and plasmonicity index (black diamonds and vertical lines) computed for selected peaks in the spectrum, labeled from a to d. The atomic structure of the cluster is shown as an inset.

DOI: 10.1021/acsphotonics.5b00688
ACS Photonics 2016, 3, 520−525

plasmonic excitation, according to the index, is the one responsible for the most intense peak, d, as expected, but also peak c shows an intense plasmonic character. This can be interpreted as a consequence of the mixed character of the excitation c, as discussed by Bernadotte et al.[11] But most importantly, this result demonstrates that the plasmonicity index provides a quantitative classification of the excitations, which works also for an excitation showing a mixed character.

Ag_{20} + Pyridine. One of the objectives of the definition of η_P is its application to hybrid systems mixing plasmonic and molecular components, where the analysis of the plasmonic properties is often not straightforward. To this aim, we considered Ag_{20} coupled to a pyridine molecule (the atomic structure is shown in the inset of Figure 4), which is a venerable

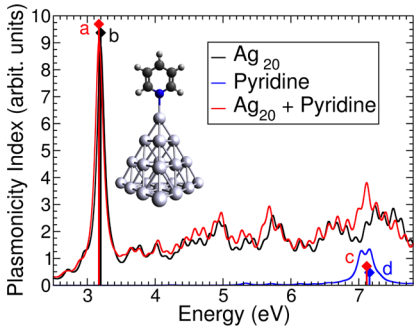

Figure 4. TDDFT absorption spectra averaged over the three spatial polarizations (in arbitrary units) of the Ag_{20} cluster (black line), the pyridine molecule (blue line), and the coupled hybrid system Ag_{20} + pyridine (red line), whose atomic structure is shown as an inset. The plasmonicity indices (diamonds and vertical lines) computed for the main peaks in the spectra of these three systems are depicted and labeled from a to d with the same color scheme for clarity.

model system for surface-enhanced spectroscopy.[34] The TDDFT absorption spectra of Ag_{20}, pyridine, and Ag_{20} + pyridine are shown in Figure 4 together with the plasmonicity index computed only for the most intense peaks in the spectra.

The index of the main absorption peak of the Ag_{20} cluster alone (peak b) is much larger compared to the index of the main absorption peak of pyridine alone (peak d). Thus, the classification in terms of the plasmonic character of the excitations provided by η_P for the isolated systems is the intuitive one. When we compute the index for the corresponding peaks in the hybrid system (peaks a and c, respectively), we find that the intuitive classification is maintained; namely, η_P of a is close to η_P of b and η_P of c is close to η_P of d, as expected.

It is worth emphasizing that we do not find intense peaks with a low plasmonicity index. As a matter of fact, by definition an excitation with an intense oscillator strength must have a large transition dipole, and, as a consequence, also the induced potential associated with the transition density turns out to be high. It follows that the plasmonicity index of that excitation is high too. In other words, the most intense peaks in the absorption spectrum are associated with excitations that are among the most plasmonic. However, other excitations may exist with an equitable plasmonic character, despite their smaller oscillator strength.

In conclusion, starting from general considerations on the interaction of matter with electromagnetic fields at the microscopic level, we rigorously defined an index that quantifies the plasmonic character of the excitations in nanostructures exploiting directly the results of first-principles simulations. This definition points out the role of the induced Coulomb potential and moves toward a fundamental understanding of the concept of a plasmon in a molecular-sized system. The different dependence with respect to the Coulomb kernel exhibited by plasmonic and nonplasmonic excitations was a key point demonstrated by Bernadotte et al.[11] and by Krauter et al.[25] by means of their scaling approach. The most important advantages of the plasmonicity index are (i) its easy readability and versatility, being a number; (ii) the fact that it does not require multiple calculations with various scaling factors on the same system; and (iii) its direct relation with the induced potential that makes it physically sound and intuitive. We numerically validated this plasmonicity index, η_P, on a Na_{20} chain and on naphthalene. We then used the index to characterize the plasmonic properties of a Ag_{20} cluster, where excitations of a mixed character have been observed, and of a paradigmatic hybrid system. The index definition allows using it also for dark excitations by exploiting the transition densities obtained from the Casida equation, although in this work the analysis has been limited to optically active excitations accessible by linear response TDDFT. The simplicity of the index is promising for its extension to other frameworks, such as other quantum and (semi)classical approaches. An open question regards the use of the plasmonicity index to directly compare the excitations of different systems. The results provided by η_P allow one to gain insights into the microscopic origin of the plasmonic resonances in small isolated and hybrid nanostructures, thus paving the way for applications to more complex systems whose plasmonic properties are not easily predictable a priori.

METHODS

The electronic structures and absorption spectra of all the investigated systems have been obtained from first-principles by means of (TD)DFT simulations, as implemented in the QUANTUM ESPRESSO[35] (QE) suite of codes. We adopt the PBE[36] Generalized Gradient Approximation (GGA) to the exchange−correlation functional, and the electronic structure calculations are performed at the Γ point of the Brillouin zone. The plane wave energy cutoff for the single-particle states and charge densities expansions for the Na_{20} chain is 32 and 384 Ry; for naphthalene, 25 and 300 Ry; for the Ag_{20} cluster and the pyridine molecule, 33 and 396 Ry, respectively. The simulation exploits periodically repeated supercells, each containing the molecular system in central position and a suitable amount of vacuum (12 Å at least) to separate adjacent replicas in the three spatial directions. The molecular structures of our systems are relaxed under the effect of the interatomic forces, with the exception of the hybrid system, where the Ag_{20} cluster and pyridine were relaxed separately. The optical absorption spectra and the response charge densities are computed exploiting the turboTDDFT code,[37] also part of the QE distribution, which implements, in the frequency domain, the Liouville−Lanczos approach to linearized TDDFT[27] and allows for the calculation of the spectra in a relatively large energy range.

This approach provides the induced charge density n', rather than the transition density ρ_ξ required for η_P defined in eq 5. Therefore, without loss of generality, we can introduce the following function of n':

DOI: 10.1021/acsphotonics.5b00688
ACS Photonics 2016, 3, 520−525

$$\tilde{\eta}_{\mathrm{P}} = \frac{\int |v_{\mathrm{ind}}(\boldsymbol{r}, \omega_\xi)|^2 \, d^3\boldsymbol{r}}{\int |n'(\boldsymbol{r}, \omega_\xi)|^2 \, d^3\boldsymbol{r}} = \frac{\int \left| \int f_{\mathrm{Coul}}(\boldsymbol{r} - \boldsymbol{r}') \, n'(\boldsymbol{r}', \omega_\xi) \, d^3\boldsymbol{r}' \right|^2 d^3\boldsymbol{r}}{\int |n'(\boldsymbol{r}, \omega_\xi)|^2 \, d^3\boldsymbol{r}} \quad (6)$$

which represents a suitable approximation for the plasmonicity index η_{P} (see the SI for further details). $\tilde{\eta}_{\mathrm{P}}$ becomes the working definition of the plasmonicity index, and it is the quantity we actually compute throughout this work exploiting the TDDFT results. Since the TDDFT perturbation is a homogeneous electric field, $\tilde{\eta}_{\mathrm{P}}$ is defined only for optically active transitions. η_{P} can be instead more generally used for dark plasmons as well.

The TDDFT implementation we use provides both the real $\Re(n')$ and the imaginary $\Im(n')$ parts of n', polarized along the three spatial directions x, y, and z. For the calculation of the index, we exploit only the imaginary part, the one related to the absorption process. If the excitation is mainly polarized along a specific direction, as for the excitation (a) of the Na_{20} chain, we restrict the calculation of the index to that polarization. Otherwise, if more polarizations are equally relevant, as in the case of the Ag_{20} cluster, we calculate the indices for all the dominant polarizations and then we average the results. The value of the broadening constant γ adopted in the linear response calculation of n', which may affect the induced densities and thus the index $\tilde{\eta}_{\mathrm{P}}$ defined in eq 6, has been chosen small enough (~0.01 eV) to virtually give a negligible induced density overlap for the analyzed excitations.

Although it can be defined for every frequency ω, $\tilde{\eta}_{\mathrm{P}}$ has a well-defined meaning only at the resonance frequencies. Since here we focus on optically active excitations, we select the frequencies ω_ξ of interest from the analysis of the peaks in the absorption spectrum. More specifically, the energy of a peak is the energy value corresponding to the point in the TDDFT spectrum with the higher oscillator strength for that peak. The resolution of the TDDFT results is 0.007 eV, allowing all the required precision in the energy determination.

■ ASSOCIATED CONTENT

Supporting Information

The Supporting Information is available free of charge on the ACS Publications website at DOI: 10.1021/acsphotonics.5b00688.

Further details on the theory, as well as selected isosurface plots for molecular orbitals and transition densities (PDF)

■ AUTHOR INFORMATION

Corresponding Authors

*E-mail: arrigo.calzolari@nano.cnr.it.

*E-mail: stefano.corni@nano.cnr.it.

Notes

The authors declare no competing financial interest.

■ ACKNOWLEDGMENTS

Computer resources were provided by the CINECA supercomputing center at their Fermi BG/Q machine through the ISCRA C PlasmInd project. The authors would like to thank in particular Nicola Spallanzani at CINECA for computational support.

■ REFERENCES

(1) Tame, M. S.; McEnery, K. R.; Özdemir, S. ̧K.; Lee, J.; Maier, S. A.; Kim, M. S. Quantum plasmonics. *Nat. Phys.* **2013**, *9*, 329−340.

(2) Savage, K. J.; Hawkeye, M. M.; Esteban, R.; Borisov, A. G.; Aizpurua, J.; Baumberg, J. J. Revealing the quantum regime in tunnelling plasmonics. *Nature* **2012**, *491*, 574−577.

(3) Linic, S.; Aslam, U.; Boerigter, C.; Morabito, M. Photochemical transformations on plasmonic metal nanoparticles. *Nat. Mater.* **2015**, *14*, 567−576.

(4) García de Abajo, F. J.; Manjavacas, A. Plasmonics in atomically thin materials. *Faraday Discuss.* **2015**, *178*, 87−107.

(5) Alonso-González, P.; Nikitin, A. Y.; Golmar, F.; Centeno, A.; Pesquera, A.; Vélez, S.; Chen, J.; Navickaite, G.; Koppens, F.; Zurutuza, A.; Casanova, F.; Hueso, L. E.; Hillenbrand, R. Controlling graphene plasmons with resonant metal antennas and spatial conductivity patterns. *Science* **2014**, *344*, 1369−1373.

(6) Halas, N. J.; Lal, S.; Chang, W.-S.; Link, S.; Nordlander, P. Plasmons in strongly coupled metallic nanostructures. *Chem. Rev.* **2011**, *111*, 3913−3961.

(7) Li, W.; Coppens, Z. J.; Besteiro, L. V.; Wang, W.; Govorov, A. O.; Valentine, J. Circularly polarized light detection with hot electrons in chiral plasmonic metamaterials. *Nat. Commun.* **2015**, *6*, 8379.

(8) Zheng, B. Y.; Wang, Y.; Nordlander, P.; Halas, N. J. Color-selective and CMOS-compatible photodetection based on aluminum plasmonics. *Adv. Mater.* **2014**, *26*, 6318−6323.

(9) Atwater, H. A.; Polman, A. Plasmonics for improved photovoltaic devices. *Nat. Mater.* **2010**, *9*, 205−213.

(10) Mayer, K. M.; Hafner, J. H. Localized surface plasmon resonance sensors. *Chem. Rev.* **2011**, *111*, 3828−3857.

(11) Bernadotte, S.; Evers, F.; Jacob, C. R. Plasmons in molecules. *J. Phys. Chem. C* **2013**, *117*, 1863−1878.

(12) García de Abajo, F. J.; Sapienza, R.; Noginov, M.; Benz, F.; Baumberg, J.; Maier, S.; Graham, D.; Aizpurua, J.; Ebbesen, T.; Pinchuk, A.; Khurgin, J.; Matczyszyn, K.; Hugall, J. T.; van Hulst, N.; Dawson, P.; Roberts, C.; Nielsen, M.; Bursi, L.; Flatté, M.; Yi, J.; Hess, O.; Engheta, N.; Brongersma, M.; Podolskiy, V.; Shalaev, V.; Narimanov, E.; Zayats, A. Plasmonic and new plasmonic materials: general discussion. *Faraday Discuss.* **2015**, *178*, 123−149.

(13) Kreibig, U.; Vollmer, M. *Optical Properties of Metal Clusters*; Springer series in material science, Vol. *25*; Springer: Berlin, 1995.

(14) Thongrattanasiri, S.; Manjavacas, A.; García de Abajo, F. J. Quantum finite-size effects in graphene plasmons. *ACS Nano* **2012**, *6*, 1766−1775.

(15) Zhang, P.; Feist, J.; Rubio, A.; García-González, P.; García-Vidal, F. J. Ab initio nanoplasmonics: the impact of atomic structure. *Phys. Rev. B: Condens. Matter Mater. Phys.* **2014**, *90*, 161407R.

(16) Barbry, M.; Koval, P.; Marchesin, F.; Esteban, R.; Borisov, A. G.; Aizpurua, J.; Sánchez-Portal, D. Atomistic near-field nanoplasmonics: reaching atomic-scale resolution in nanooptics. *Nano Lett.* **2015**, *15*, 3410−3419.

(17) Kümmel, S.; Andrae, K.; Reinhard, P.-G. Collectivity in the optical response of small metal clusters. *Appl. Phys. B: Lasers Opt.* **2001**, *73*, 293−297.

(18) Zheng, B. Y.; Zhao, H.; Manjavacas, A.; McClain, M.; Nordlander, P.; Halas, N. J. Distinguishing between plasmon-induced and photoexcited carriers in a device geometry. *Nat. Commun.* **2015**, *6*, 7797.

(19) Guidez, E. B.; Aikens, C. M. Origin and TDDFT benchmarking of the plasmon resonance in acenes. *J. Phys. Chem. C* **2013**, *117*, 21466−21475.

(20) Townsend, E.; Bryant, G. W. Which resonances in small metallic nanoparticles are plasmonic? *J. Opt.* **2014**, *16*, 114022.

(21) Guidez, E. B.; Aikens, C. M. Quantum mechanical origin of the plasmon: from molecular systems to nanoparticles. *Nanoscale* **2014**, *6*, 11512−11527.

(22) Bursi, L.; Calzolari, A.; Corni, S.; Molinari, E. Light-induced field enhancement in nanoscale systems from first-principles: the case of polyacenes. *ACS Photonics* **2014**, *1*, 1049−1058.

DOI: 10.1021/acsphotonics.5b00688
ACS Photonics 2016, 3, 520−525

(23) Krauter, C. M.; Schirmer, J.; Jacob, C. R.; Pernpointner, M.; Dreuw, A. Plasmons in molecules: microscopic characterization based on orbital transitions and momentum conservation. *J. Chem. Phys.* **2014**, *141*, 104101.
(24) Townsend, E.; Debrecht, A.; Bryant, G. W. Approaching the quantum limit for nanoplasmonics. *J. Mater. Res.* **2015**, *30*, 2389−2399.
(25) Krauter, C. M.; Bernadotte, S.; Jacob, C. R.; Pernpointner, M.; Dreuw, A. Identification of plasmons in molecules with scaled ab initio approaches. *J. Phys. Chem. C* **2015**, *119*, 24564−24573.
(26) Fetter, A. L.; Walecka, J. D. *Quantum Theory of Many-Particle Systems*; Dover Publications: Mineola, NY, 2003.
(27) Marques, M. A. L.; Maitra, N. T.; Nogueira, F. M. S.; Gross, E. K. U.; Rubio, A., Eds. *Fundamentals of Time-Dependent Density Functional Theory*; Springer series: Lecture Notes in Physics, Vol. *837*; Springer: Berlin, 2012.
(28) della Sala, F.; D'Agostino, S. *Handbook of Molecular Plasmonics*; Pan Stanford Publishing Pte. Ltd., 2013.
(29) Egri, I. Excitons and plasmons in metals, semiconductors and insulators: a unified approach. *Phys. Rep.* **1985**, *119*, 363−402.
(30) Yan, J.; Yuan, Z.; Gao, S. End and central plasmon resonances in linear atomic chains. *Phys. Rev. Lett.* **2007**, *98*, 216602.
(31) Chen, M.; Dyer, J. E.; Li, K.; Dixon, D. A. Prediction of structures and atomization energies of small silver clusters, $(Ag)_n$, $n < 100$. *J. Phys. Chem. A* **2013**, *117*, 8298−8313.
(32) Manjavacas, A.; Marchesin, F.; Thongrattanasiri, S.; Koval, P.; Nordlander, P.; Sánchez-Portal, D.; García de Abajo, F. J. Tunable molecular plasmons in polycyclic aromatic hydrocarbons. *ACS Nano* **2013**, *7*, 3635−3643.
(33) Lauchner, A.; Schlather, A. E.; Manjavacas, A.; Cui, Y.; McClain, M. J.; Stec, G. J.; García de Abajo, F. J.; Nordlander, P.; Halas, N. J. Molecular plasmonics. *Nano Lett.* **2015**, *15*, 6208−6214.
(34) Zhao, L.; Jensen, L.; Schatz, G. C. Pyridine-Ag20 cluster: a model system for studying surface-enhanced Raman scattering. *J. Am. Chem. Soc.* **2006**, *128*, 2911−2919.
(35) Giannozzi, P.; Baroni, S.; Bonini, N.; Calandra, M.; Car, R.; Cavazzoni, C.; Ceresoli, D.; Chiarotti, G. L.; Cococcioni, M.; Dabo, I.; Dal Corso, A.; de Gironcoli, S.; Fabris, S.; Fratesi, G.; Gebauer, R.; Gerstmann, U.; Gougoussis, C.; Kokalj, A.; Lazzeri, M.; Martin-Samos, L.; Marzari, N.; Mauri, F.; Mazzarello, R.; Paolini, S.; Pasquarello, A.; Paulatto, L.; Sbraccia, C.; Scandolo, S.; Sclauzero, G.; Seitsonen, A. P.; Smogunov, A.; Umari, P.; Wentzcovitch, R. M. QUANTUM ESPRESSO: a modular and open-source software project for quantum simulations of materials. *J. Phys.: Condens. Matter* **2009**, *21*, 395502.
(36) Perdew, J.; Burke, K.; Ernzerhof, M. Generalized gradient approximation made simple. *Phys. Rev. Lett.* **1996**, *77*, 3865−3868.
(37) Ge, X.; Binnie, S. J.; Rocca, D.; Gebauer, R.; Baroni, S. turboTDDFT 2.0 - Hybrid functionals and new algorithms within time-dependent density-functional perturbation theory. *Comput. Phys. Commun.* **2014**, *185*, 2080−2089.

DOI: 10.1021/acsphotonics.5b00688
ACS Photonics 2016, 3, 520−525